STRAGGLING OF ENERGY LOSS FOR ELECTRONS TRANSMITTED THROUGH ALUMINUM*

C. M. Kwei
Institute of Electronics
National Chiao Tung University
Hsinchu, Taiwan 300
Republic of China

Summary

A study of the energy loss spectra of electrons transmitted through aluminum foil was carried out. Inelastic interactions of electrons with the conduction band as well as inner shells of aluminum have been considered. Energy loss spectra were computed for several monoenergetic electron sources and film thicknesses. Theoretical results have been compared with available experimental data.

Introduction

Electron mean free paths, stopping powers, and ranges are important parameters for experimental and theoretical studies in a wide variety of applied areas. Information generated on these quantities are available for electron energies less than 10 keV for many materials.[1] Such information together with the Bethe theory[2] for electron energies $\geq$10 keV should provide useful guides for order of magnitude estimates in electron penetration studies. To completely describe the penetration phenomena one must also consider stragglings of the above mean quantities. These stragglings are due to the statisitical fluctuations of the frequency and energy loss of collisions along the electron track.

In this paper we calculate the energy loss straggling of electrons transmitted through aluminum foils. This quantity represents the energy loss distribution of electrons that have traveled a given pathlength under identical initial conditions. Our emphasis will be on the energy loss region where plasmon excitations are most important. The theory and models used in this work will be described in the next few sections. Theoretical results of our calculations will be compared with available experimental data.

Straggling theory

The energy loss straggling may be described by a distribution function $f(E,x,\omega)d\omega$; it represents the probability that an electron of energy E will have lost an energy ω on penetrating a thickness x of the medium. This function obeys the transport equation[3-5]

$$\frac{\partial f(E,x,\omega)}{\partial x} = \int_0^\infty f(E,x,\omega-\omega')\frac{d\mu}{d\omega'}(E-\omega+\omega',\omega')d\omega' - \int_0^\infty f(E,x,\omega)\frac{d\mu}{d\omega'}(E-\omega,\omega')d\omega' + \delta(E-E_0)\delta(x), \quad (1)$$

where $d\mu(E,\omega)/d\omega$ is the differential inverse mean free path (DIMFP) for an electron of energy E to lose the energy ω. Dirac delta functions in Eq.(1) indicate that a monoenergetic electron source of energy E_0 constitutes the point of zero pathlength. Here we allow the distribution function to vary with the energy of the degraded electrons, an effect which is important for low energy electrons.

Equation (1) can be solved using the convolution method. Setting

$$f(E,x_1+x_2,\omega)=\int_0^\omega f(E,x_1,\omega-\omega')f(E-\omega+\omega',x_2,\omega')d\omega', \quad (2)$$

we can compute the distribution of electrons which lost energy ω in thickness x_1+x_2 by the convolution of the distribution which lost energy $\omega-\omega'$ in x_1 with the distribution which lost energy ω' in x_2. If we start with a thickness x for which the probability of a collision is very small, the left-hand side of Eq.(1) may be approximated by

$$\frac{\partial f(E,x,\omega)}{\partial x} \approx \frac{f(E,x,\omega)-\delta(\omega)}{x}. \quad (3)$$

Substituting this relation into Eq.(1), we obtain by iteration an approximate solution

$$f^{(n)}(E,x,\omega)=\delta(\omega)+x\int_0^\infty f^{(n-1)}(E,x,\omega-\omega')\frac{d\mu}{d\omega'}(E-\omega+\omega',\omega')d\omega' - xf^{(n-1)}(E,x,\omega)\mu(E-\omega), \quad (4)$$

where $\mu(E)=\int_0^\infty \frac{d\mu}{d\omega}(E,\omega)d\omega$ is the inverse mean free path for electrons of energy E. A few lower-order approximate solutions are

$$f^{(0)}(E,x,\omega)=\delta(\omega),$$
$$f^{(1)}(E,x,\omega)=\delta(\omega)\{1-x\mu(E)\}+x\frac{d\mu}{d\omega}(E,\omega),$$
$$f^{(2)}(E,x,\omega)=\delta(\omega)\{1-x\mu(E)+x^2\mu^2(E)\}+x\frac{d\mu}{d\omega}(E,\omega)\{1-x\mu(E)-x\mu(E-\omega)\}+x^2\int\frac{d\mu}{d\omega'}(E,\omega-\omega')\frac{d\mu}{d\omega'}(E-\omega+\omega',\omega')d\omega'. \quad (5)$$

In general, the nth-order solution may be written as

$$f^{(n)}(E,x,\omega)=\delta(\omega)p^{(n)}(E,x)+q^{(n)}(E,x,\omega), \quad (6)$$

where

$$p^{(n)}(E,x)=1-x\mu(E)p^{(n-1)}(E,x), \quad (7)$$

$$q^{(n)}(E,x,\omega)=x\frac{d\mu}{d\omega}(E,\omega)p^{(n-1)}(E,x)-x\mu(E-\omega)q^{(n-1)}(E,x,\omega)+x\int\frac{d\mu}{d\omega'}(E-\omega+\omega',\omega')q^{(n-1)}(E,x,\omega-\omega')d\omega', \quad (8)$$

and

$$p^{(0)}(E,x)=1, \quad (9)$$

$$q^{(0)}(E,x,\omega)=0. \quad (10)$$

For simplicity, the convolution technique is applied for segments of equal thickness. On choosing $x_1=x_2=x$, we can calculate $f(E,t,\omega)$ for any desired value of thickness t. Substituting Eq.(6) into Eq.(2), we obtain after n convolutions

$$f(E,2^nx,\omega)=C^{2^n}(E,x)\delta(\omega)+F_n(E,x,\omega), \quad (11)$$

where

$$C(E,x)=p^{(n)}(E,x), \quad (12)$$

$$F_0(E,x,\omega)=q^{(n)}(E,x,\omega), \quad (13)$$

*Work supported by the National Science council of the Republic of China.

0018-9499/81/1200-4172$00.75

and

$$F_n(E,x,\omega)=\left(C^{2^{n-1}}(E-\omega,x)+C^{2^{n-1}}(E,x)\right)F_{n-1}(E,x,\omega)$$
$$+\int_0^{\omega} F_{n-1}(E,x,\omega-\omega')F_{n-1}(E-\omega+\omega',x,\omega')d\omega'. \quad (14)$$

These equations can be solved numerically.

The distribution function described above contains two variables, i.e., distance and energy. In many applications it is necessary to know the single variable distribution of simple energy degradation. This is done by averaging out the distribution function in Eq.(1) over the distance. On defining

$$\phi(\omega)=\int_{-\infty}^{\infty} f(E,x,E-\omega)dx, \quad (15)$$

it is easy to show that

$$\phi(E)\mu(E)=\int_0^{\infty}\phi(E+\omega)\frac{d\mu}{d\omega}(E+\omega,\omega)d\omega+\delta(E-E_0). \quad (16)$$

The function $\phi(E)$ is usually referred to as the electron slowing-down spectrum. It represents the average pathlength traveled by the electron while its energy lies between E+dE and E in the course of its slowing-down.[6] Note that Eq.(16) does not include the contribution due to the generation of secondary electrons. Numerical methods used to solve this equation were given elsewhere in detail.[6]

Differential Inverse Mean Free Path

The basic component in the straggling theory is the DIMFP for inelastic interactions of an electron with the medium. For the contribution from the conduction band, this quantity may be given in the Born approximation as

$$\frac{d\mu}{d\omega}(E,\omega)=\frac{1}{\pi E}\int_{k_-}^{k_+}\frac{dk}{k}\,\mathrm{Im}\left(\frac{-1}{\varepsilon(k,\omega)}\right), \quad (17)$$

where $\hbar k_{\pm}=\sqrt{2}(\sqrt{E}\pm\sqrt{E-\omega})$, k and ω are, respectively, the momentum transfer and the energy transfer, and $\varepsilon(k,\omega)$ is the scalar dielectric function of the electron gas formed by the conduction band electrons. Here we express all physical quantities in atomic units (a.u.).

Generally, there are two types of excitation for a given momentum transfer k. These are shown in Fig.1.

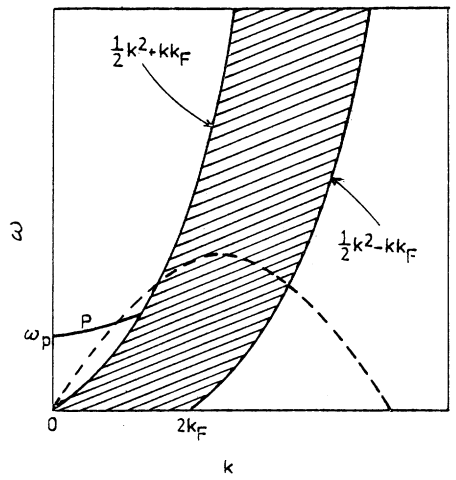

Fig.1. Spectrum of excitation energies *vs.* momentum transfer k for an electron gas. The shaded region is that in which single electron-hole excitation is possible. The solid curve labeled P is the plasmon excitation line. The broken curve shows an energy momentum conservation curve and k_F is the Fermi momentum.

Plasmon excitations are most important for small k, whereas single electron-hole excitations dominate exclusively for large k. For the present applications, we use the Drude dielectric function to describe plasmon excitations and the Lindhard dielectric function for single electron-hole excitations. Thus we let

$$\varepsilon(k,\omega)=\begin{cases}\varepsilon_D(k,\omega), & \text{for } \omega>\frac{k^2}{2}+kk_F\\ \varepsilon_L(k,\omega), & \text{for } \omega<\frac{k^2}{2}+kk_F\end{cases} \quad (18)$$

where k_F is the Fermi momentum. Actually, there occurs a maximum momentum transfer in $\varepsilon_D(k,\omega)$, above which the plasmons damp into single electron-hole pairs. This can be seen from studies of the sum rule

$$\int_0^{\infty}\omega\,\mathrm{Im}\left(\frac{-1}{\varepsilon(k,\omega)}\right)d\omega=2\pi^2\eta_{eff}, \quad (19)$$

where η_{eff} is the effective number of conduction electrons per unit volume. The departure of η_{eff} from the theoretically predicted valence electron density is due to the shielding of valence electrons by the polarization of core electrons and the coupling of oscillator strength between core and valence electrons. Using generalized oscillator strengths for inner shells calculated from the Hartree-Slater model, Smith and Shiles[7] have determined that 3.1 valence electrons contributed to the oscillator strength for excitations of the conduction band of aluminum. However, if we substitute the Lindhard dielectric function to the left-hand side of Eq.(19), we find that the contribution to the oscillator strength due to single electron-hole excitations varies with the momentum transfer. Figure 2 shows the single electron-hole contribution to the effective number of conduction electrons per Al atom, N_s, as a function of momentum transfer. It indicates a complete consumption of oscillator strength due to the excitation of single electron-holes at momentum transfers greater than $\sim$0.7 a.u.

The imaginary part of the negative reciprocal of the complex Drude dielectric function is given by

$$\mathrm{Im}\left(\frac{-1}{\varepsilon_D(k,\omega)}\right)=\frac{A(k)\omega_p^2\,\omega\,\gamma}{\left(\omega^2-\omega_p^2(k)\right)^2+\gamma^2\omega^2}, \quad (20)$$

where ω_p is the plasma frequency, γ is a damping constant, $\omega_p(k)$ represents the plasma dispersion relation, and A(k) is the momentum dependent oscillator strength which is determined from Eq.(19) and the data presented in Fig.2. Results calculated for A(k) are also plotted in Fig.2. It is seen that the oscillator strength for plasmon excitations decreases from unity at k=0 to zero at $k\sim 0.7$ a.u. Here we have used γ=1 eV[8] and the relation[9]

$$\omega_p(k)=\omega_p+0.4k^2+0.2k^4 \quad (21)$$

from the experimental measurements.

Results and Discussion

Figure 3 shows some representative results of the DIMFP for plasmon excitations as a function of energy transfer for several values of incident electron energies. Calculations of the DIMFP for single electron-hole excitations have been made previously using the Lindhard dielectric function.[6] Results corresponding to the conduction band of aluminum taking 3.1 conduction electrons per Al atom are shown in Fig.4. Other contribution to the DIMFP from the ionization of inner

shells are available elsewhere.[6]

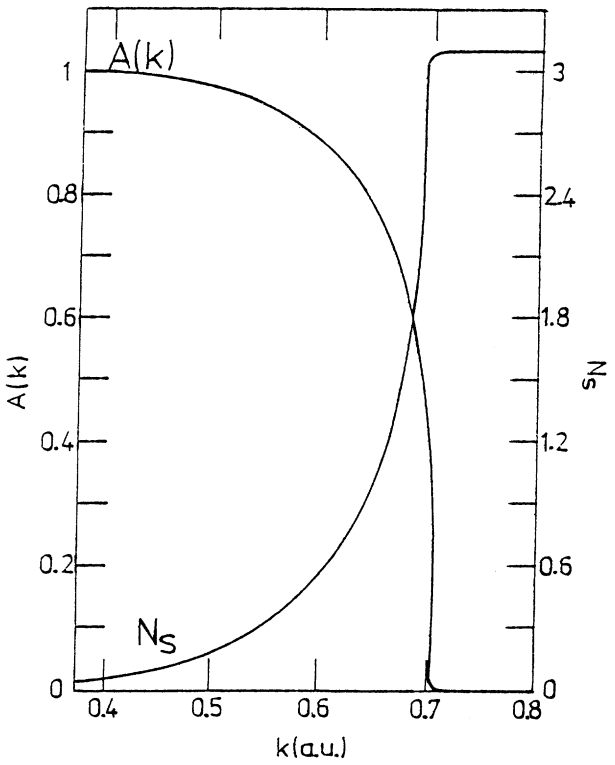

Fig.2. A plot of the single electron-hole contribution to the effective number of conduction electrons per Al atom (right ordinate) as a function of momentum transfer. The oscillator strength factor, A(k), in Eq.(20) is plotted with the left ordinate scale.

DIMFP calculated above were used to compute the energy loss straggling function for electron transmitted through aluminum foils. In Fig.5 we plot the result of the straggling function for a 2580 Å foil and a 20 keV incident electron. This distribution is compared with experimental data measured by Marton *et al.*[10] The peaks in the spectrum correspond to energy losses due to the generation of one, two, three, etc., plasmons in successions. After several fluctuations as energy loss increases, the spectrum becomes fairly smooth. The broad continuum underlying the discrete loss spectrum may be composed of overlapping tails from the discrete loss peaks. Figure 6 is a plot of the straggling function computed for electrons of 1.8 keV transmitted through aluminum foil of 220 Å thickness. One sees again that the spectrum consists of the typical plasmon peaks at low energy losses. The overall asymmetric straggling distribution about a most probable value is due to the fact that smaller energy losses are more probable than the large losses. Because of the asymmetric behavior, the average energy loss for transmitted electrons may be quite different from the most probable energy loss. In the present case, $\varpi = 2.5 \sim 3\omega_{mp}$. A sketch of the experimental data of Fitting[11] is also included in the same figure for comparisons. Here the resolution of energy in the experiment seems not good enough to show detailed structure in the spectrum at small energy losses. Figure 7 shows a similar plot for electrons of 1 keV transmitted through aluminum of 220 Å thickness. The plasmon peaks at low energy losses are not so manifest here. The asymmetric straggling distribution has the characteristics of becoming broad and shifted to higher energy losses. This is confirmed by the result that the energy loss per unit pathlength at 1 keV is greater than that at 1.8 keV.[1]

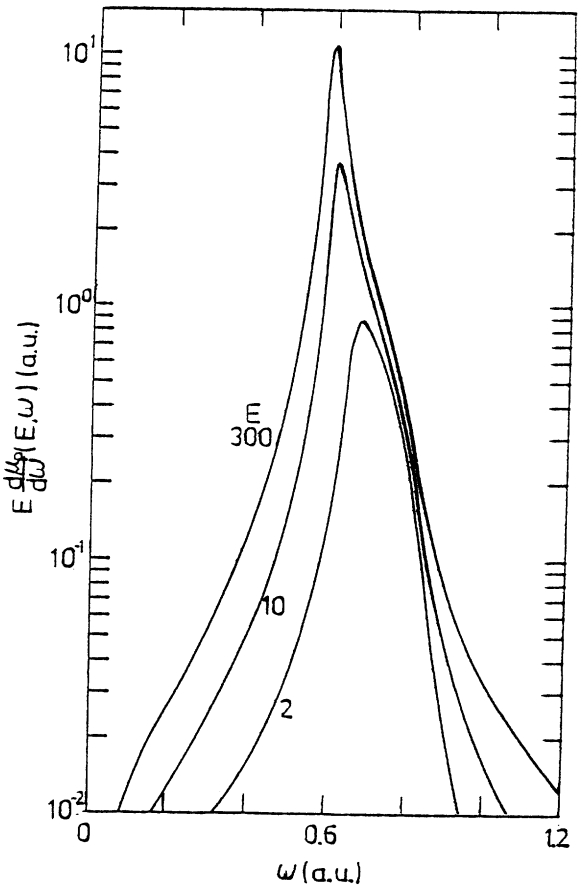

Fig.3. Representation of $E\frac{d\mu_p}{d\omega}(E,\omega)$ as a function of ω for several values of electron energy E. Here $\frac{d\mu_p}{d\omega}$ is the DIMFP for plasmon excitations in aluminum.

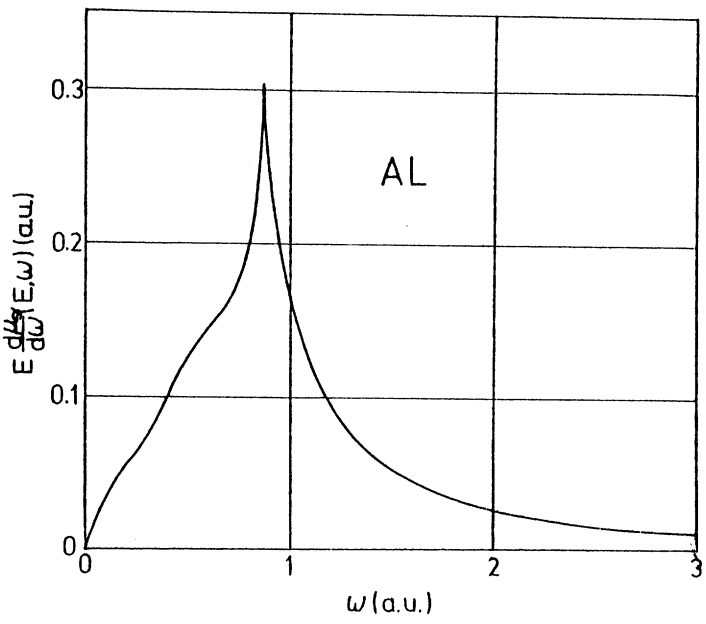

Fig.4. A plot of $E\frac{d\mu_s}{d\omega}(E,\omega)$ *vs.* ω for an electron gas corresponding to the conduction band of Al. Here $\frac{d\mu_s}{d\omega}$ is the DIMFP for single electron-hole excitations.

Finally, we plot in Fig.8 the electron slowing-down spectrum as a function of electron energy loss due to the source of monoenergetic electrons with the energy $E_0 = 1000$ eV. This spectrum corresponds to a source density normalized to one electron emitted per unit volume per unit time. It may be used to calculate the yield of reactions produced by an electron during its slowing-down.

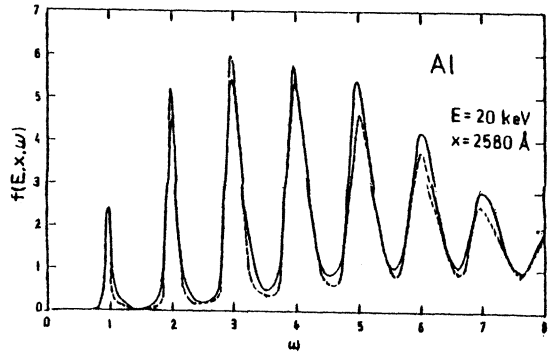

Fig.5. A plot of the straggling function *vs.* energy loss for a 20 keV electron and 2580 Å Al foil. The broken curve is the results of the experimental data of Marton *et al.*[10]

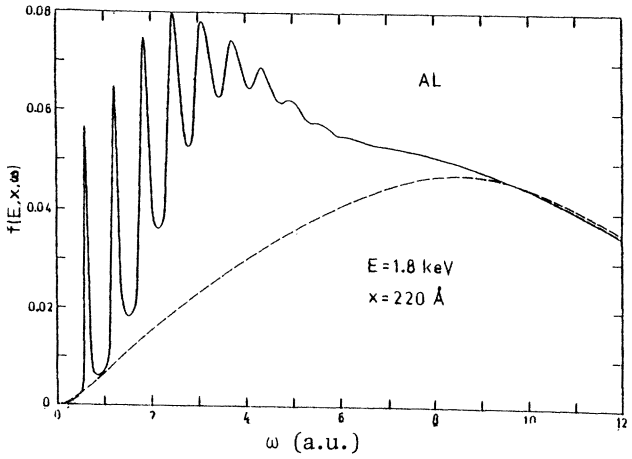

Fig.6. A plot of the straggling function *vs.* energy loss for a 1.8 keV electron and 220 Å Al foil. A sketch of the experimental data of Fitting[11] is included for comparisons.

Acknowledgments

The author wishes to express cordial thanks to Dr. C. J. Tung for many helpful discussions. The assistance from the Computing Center of National Chiao Tung University is gratefully acknowledged.

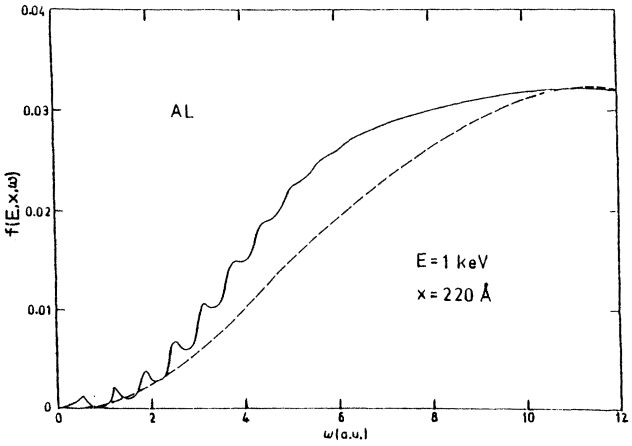

Fig.7. A plot of the straggling function *vs.* energy loss for a 1 keV electron and 220 Å Al foil. A sketch of the experimental data of Fitting[11] is included for comparisons.

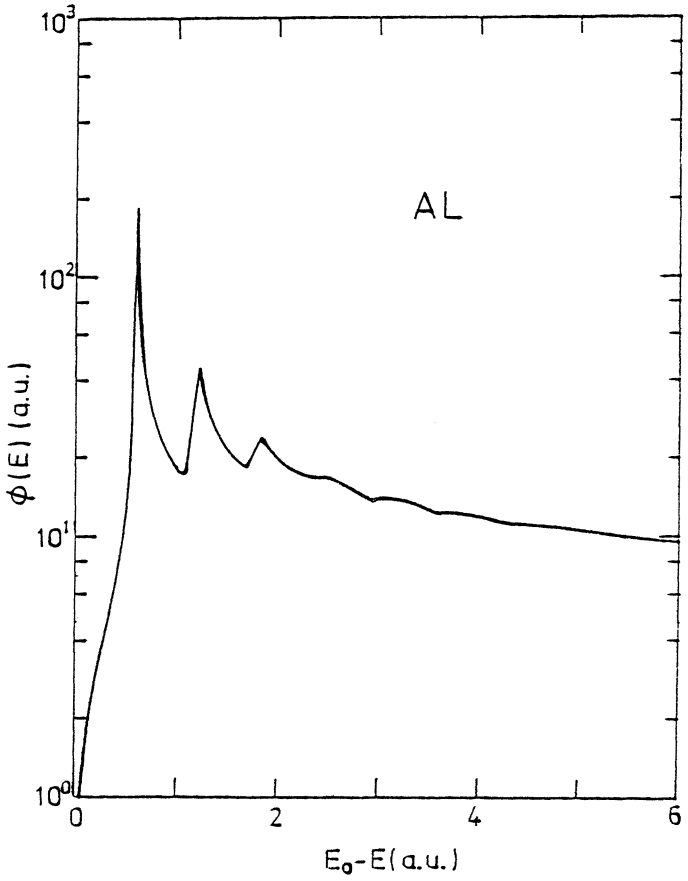

Fig.8. A plot of the electron slowing-down spectrum in aluminum against electron energy loss, $E_0 - E$, for a monoenergetic electron source with energy $E_0 = 1$ keV.

References

1. See, e.g., C. J. Tung, J. C. Ashley and R. H. Ritchie, *IEEE Trans. Nucl. Sci.* NS-26, 4874 (1979), and references contained therein.

2. L. Pages, *et al. Atomic Data* 4, 1 (1972).

3. C. J. Tung and C. M. Kwei, *Thin Solid Films* 75, 371 (1981).

4. H. Bichsel and R. P. Saxon, *Phys. Rev. A* 11, 1286 (1975).

5. J. C. Ashley, J. J. Cowan, R. H. Ritchie, V. E. Anderson and J. Hoelzl, *Thin Solid Films* 60, 361 (1978).

6. C. J. Tung and R. H. Ritchie, *Phys. Rev. B* 16, 4302 (1977).

7. D. Y. Smith and E. Shiles, *Phys. Rev. B* 17, 4689 (1978).

8. J. C. Ashley and R. H. Ritchie, *Phys. Stat. Sol. (b)* 83, K159 (1977).

9. N. Swanson and C. J. Powell, *Phys. Rev.* 145, 197 (1966).

10. L. Marton, J. A. Simpson, H. A. Fowler and N. Swanson, *Phys. Rev.* 126, 182 (1962).

11. H. J. Fitting, *Phys. Stat. Sol. (a)* 26, 525 (1974).